Terahertz Responsivity Calculation of Unipolar Diodes Based on Transistor Channels Model

Abdel Majid. Mammeri, F. Z Mahi
Institute of Science and Technology
university of Bechar
Algeria
fati_zo_mahi2002@yahoo.fr

H. Marinchio, C. Palermo and L. Varani
Institute of electronic and systems
university of Montpellier 2
France
fati64@live.com

Abstract: In this contribution, we propose an analytical approach for the Responsivity calculation of the nanochannel diodes. The analytical model is based on the total current of HEMT transistor channels in Ref. [1] with distance channel-gate tends to infinity. This consideration (ungated transistor) leads to determine the admittance at the nanochannel diode terminals. The admittance elements are then used to calculate the impedance and therefore the Responsivity of the diode. The impedance and the Responsivity exhibit resonances in the terahertz domain which are discussed as functions of the device geometry, operating temperature and applied voltage. Moreover, the high quality resonance can improve the detection of their frequencies. Indeed, the analysis of the Responsivity generated from the power signal is useful for the optimization of Terahertz detectors applications. The results will be compared with the admittance calculated by using the hydrodynamic approach in Ref. [2] where the small-signal elements of homogenous diodes in Terahertz frequencies are determined.

Key–Words: Unipolair diodes (SSD), Terahertz (THz), resonances, Responsivity analytical model.

1 Introduction

In the last years, the nanodiodes have shown a great potential application for the terahertz frequency range [3]. Moreover, the unipolar nanodiode has shown experimentally a good Responsivity for a microwave voltage [4]. Therefore, many researchs are supported for the realization of InGaAs nanochannel diode described in Ref. [5]. In particular, the finite-element simulations in Ref [4] and the experimental methode [6] are using to improve the responsivity of the nano diodes.

In this contribution, the nanochannel diode with high electrons mobility based on InGaAs material, obtained by an ungated transistors structure (for high distance channel-gate), presents a plasma resonance in the Terahertz frequency range [2]. The analytical model based on the total current along the channel of HEMT transistor in Ref. [7], with the consideration channel-gate distance tends to infinity, is used for the channel diodes characterization. In the same direction, the analytical model in Ref. [1] gives a partial description of an ungated transistor response which corresponding to the study in this paper (channel diode for high distance channel-gate). Indeed, when we increase the distance channel-gate the behavior of the transistor tends more and more to behave as a diode. This consideration simplifies the transistor to a channel diode and therefore the transistor analytical model becomes useful for the calculation of equivalent circuit elements of this diode in high-frequency regime. Then, the admittance elements can be used to obtain the impedance and therefore the Responsivity of a channel diode.

The impedance elements are studied and interpreted as a function of the diode length and operating temperature where the Responsivity is analyzed as a function of the applied voltage. The discussion improves the dynamic regime of the diode in terahertz frequency range. Finaly, the analytical results of the diode impedance will be compared to the Hydrodynamic calculations in Ref. [2].

1.1 Analytical model of channel diode

We consider an unipolar diode which is similar to that studied in Ref. [7] when the gate is moved away from the channel (d tends to infinity). Moreover, this consideration ($d \to \infty$) leads to use the analytical model described in Ref. [7] for the terahertz characterization of nanochannel diode. The diode with high doped structure n^+ reported schematically in Figure 1 where the L is the length and δ is the thickness of diode.

In extension, the currents-potentials relation at source and drain transistor terminals calculated by equation (4) in Ref. [7] and expressed above by equation (7) in Ref. [1] is rewritten as:

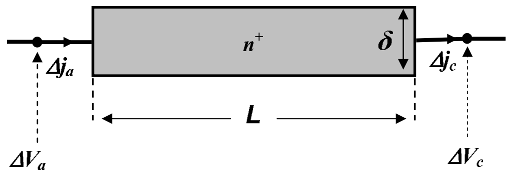

Figure 1: Structure representation of an high doped unipolar diode n^+ of length L and thickness δ. The amplitudes of the anode and cathode are ΔV_a and ΔV_c respectively.

$$\begin{bmatrix} \Delta j_s(\omega) \\ \Delta j_d(\omega) \end{bmatrix} = \frac{G\beta}{sh\beta L} \begin{pmatrix} ch\beta L & -1 \\ 1 & -ch\beta L \end{pmatrix} \begin{bmatrix} \Delta V_s(\omega) \\ \Delta V_d(\omega) \end{bmatrix} \tag{1}$$

Where the terms $\beta^2 = \lambda^2 \left[i\omega \left(i\omega + \nu \right) \alpha / \omega_p^2 \right]$ and $\lambda = \sqrt{1/d\delta}$ are strongly related to the distance channel-gate d. When we introduce the consideration $d \to \infty$ in equation (1), the anode/cathode current-potential relation of channel diode is achieved. As follows, the increase of the distance at the infinity limit ($d \to \infty$) in equation (1) remains the terms λ and β equal to zero and therefore the term $ch\beta L$ equals to 1 and $sh\beta L = L$. This is accompanied by an approximated current-potential relation at the anode and cathode terminals in absence of thermal noise as:

$$\begin{bmatrix} \Delta j_a(\omega) \\ \Delta j_c(\omega) \end{bmatrix} = \frac{G}{L} \begin{pmatrix} 1 & -1 \\ 1 & -1 \end{pmatrix} \begin{bmatrix} \Delta V_a(\omega) \\ \Delta V_c(\omega) \end{bmatrix} \tag{2}$$

The matrix elements in equation (2) gives the same admittance expressions at the cathode, anode and cthode-anode contacts as $|Y_{aa}| = |Y_{cc}| = |Y_{ac}| = |Y_{ca}| = \frac{G}{L}$, respectively. Where $G = \epsilon_c \epsilon_0 \omega_p^2 \alpha^{-1} / \left(i\omega + \nu \right)$, $\alpha = \omega_p^2 / \left(\omega_p^2 + i\omega(i\omega + \nu) \right)$, $\omega_p = \sqrt{e^2 n_0 / \epsilon_c \epsilon_0 m^*}$, ν is the relaxation rate of bulk semiconductor and n_0 is the electron concentration. The equation (2) presents the basis for the calculation of the diode impedance components in terahertz frequency as:

$$\widehat{Y}(\omega) = \widehat{Z}^{-1}(\omega) \tag{3}$$

where $\widehat{Y}(\omega)$ and $\widehat{Z}(\omega)$ are the admittance and impedance matrices, respectively.

When a sinusoidal voltage $V = V_{DC} + V_0 cos(\omega t)$ applied to the diode the current response $j(t)$ is rectified to the spectra current $\Delta j(\omega)$ obtained by using equation (2). In this case, the intrinsic Responsivity is determined by the rectified current $\Delta j(\omega)$ and the resistance of the diode R as:

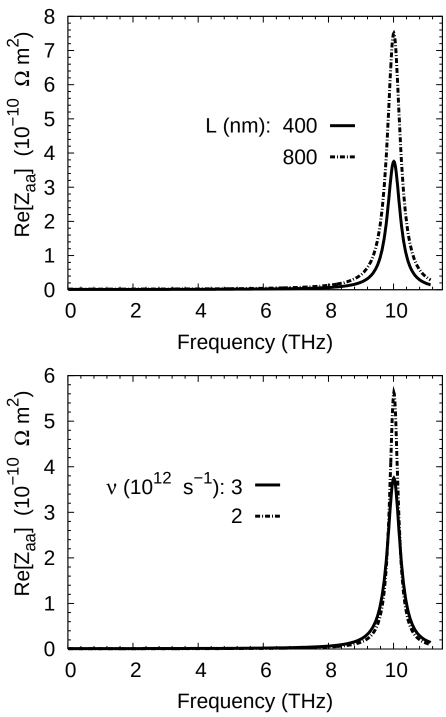

Figure 2: Real part of impedance as functions of the frequency for the reported lengths L and relaxations rate ν.

$$S_{int}(\omega) = \frac{\Delta j(\omega) \times R(\omega)}{Re[V_0^2 / 2Z(\omega)]} \tag{4}$$

with $R(\omega) = Re[Z(\omega)]$ resistance corresponds to the real part of the diode complex impedance $Z(\omega)$. Let us note that the impedance $Z(\omega)$ is extracted from the inverse admittance matrix described by equation (3).

2 Impedance of the nanochannel diode

We discuss, the real part of the impedance as functions of the diode parameters (length L, relaxation rate ν and doping concentration n_0). We consider a InGaAs nanochannel diode with a thickness $\delta = 15$ nm. Let us note that we present the impedance real part $Re[Z(\omega)]$, at the anode and cathode terminals, which is widely used for the intrinsic Responsivity calculations. The figure 2 illustrates the modification introduced by the length L and the relaxation rate ν on the real part of impedance when the diode electron concentration is $n_0 = 8 \times 10^{17}$ cm^{-3}.

In figure 2, we observe the appearance of one resonance peak near 10 THz corresponding to the plasma frequency ω_p. Indeed, the resonance frequency of

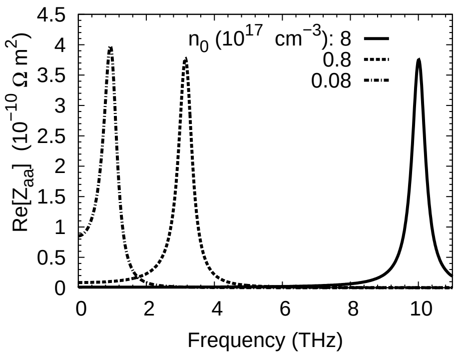

Figure 3: Real part of impedance as functions of the frequency for the reported electron concentration. With $L = 400$ nm, $\nu = 3{\times}10^{12}$ s^{-1}.

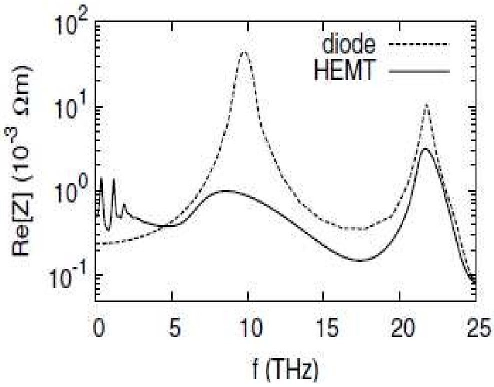

Figure 4: The real part of small-signal impedance calculated for the diode (dashed line) and HEMT transistor (solid line) under the constant-drain-current operation.

$Re[Z_{aa}]$ (near 10 THz) can be compared and interpreted by the expression [2, 8]:

$$f_p = \omega_p \frac{p}{\sqrt{\left(\frac{\lambda L}{\pi}\right)^2 + p}} \tag{5}$$

where $p = 1, 2, 3, 4..$ number of excitation. The resonance peak of diode impedance spectrum is obtained according to equation (5) when $\lambda \rightarrow 0$ (for $d \rightarrow \infty$):

$$f_{res} = \omega_p = const \tag{6}$$

Compared to the plasma resonances of the transistor admittance f_p (equation (5)), the impedance spectrum exhibits one plasma resonance f_{res} (equation (6)) explaining the absence of oscillations along the diode channel. It's more clear that the resonance peak f_{res} is related to the electron concentration n_0 through the analytic expression of ω_p. The modification introduces by the change of concentration n_0, on the appearance of the resonance peak, is reported in Fig. 3

Moreover, the amplitude of the resonance peak decreases for the decreasing of diode length at room temperature corresponds to relaxation rate $3{\times}10^{12}$ s^{-1}. In addition, we remark the displacement of the resonance peak to the low frequency for the concentration $8{\times}10^{15}$ cm^{-3} (see figure 3). Therefore, the high resonance obtained by the real part impedance is for the high doped concentration $8{\times}10^{17}$ cm^{-3}.

These results have been demonstrated by using the hydrodynamic approach in Ref. [2]. The figure 4 presents the hydrodynamic impedance calculation of the transistor and the unipolar diode when the gate is removed from the channel.

We remark that the appearance of the resonance peak is near 10 THz in dashed line corresponding to the real part of diode impedance in figure 2. It should be emphasized that the good agreement found between analytical and hydrodynamic results in the frequency range of interest.

3 Responsivity of nanochannel diode

we suppose that the dc and ac voltages are equals $V_{DC} = V_0$ and the applied voltage V is proportional to $V(t) = V_0 + V_0 cos(\omega_0 t)$. The calculations of the Responsivity will be carried out for a constant voltage and microwave voltage applied to the diode. For the first calculation, the Responsivity is determined for different fixed values of the voltage V corresponding to $2V_0, V_0 + \frac{V_0}{2}, V_0$. We extract the rectified current $\Delta j(\omega)$ at a certain voltage V form the expression $\Delta j(\omega_0) = Y(\omega)V$.

For the second calculation, we assume that the voltage takes an adiabatic variation in time $V(t) = V_0 + V_0 cos(\omega_0 t)$ where ω_0 has a finite value 10 GHz. In this case, the Responsivity is determined under a microwave voltage applied to the diode. According to the discussion of diode parameters effect on the real part of impedance, the concentration n_0 has an important effect on the frequency resonance. For this reason, we take as consideration the concentration effect for the Responsivity analysis.

Figure 5 illustrates a frequency behavior of the Responsivity at a constant voltage $V = const$ ($\omega_0 t = const$) applied to the diode terminals. The results of figure 3 consist the first step of the Responsivity calculation where $V_0 = 0.25$ V.

The figure 5 performed the diode responsivity under a constant voltage operation V, when the current flowing through the diode changes its values by a certain constant voltage. At low frequencies, the Responsivity presents the Lorentzian shape corresponding to the behavior of homogenous diode, and a peak at fre-

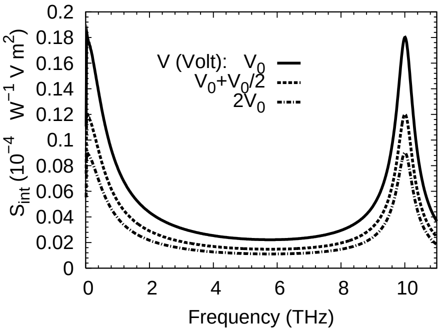

Figure 5: Intrinsic responsivity S_{int} for different fixed values of the voltage V corresponding to different phases of the ac component $V(t) = V_0 + V_0 cos(\omega_0 t)$ ($\omega_0 t = 0, \pi/3, \pi/2$). With $V_0 = 0.25$ V, $L = 400$ nm, $\nu = 3{\times}10^{12}$ s^{-1} and electron concentration $n_0 = 8{\times}10^{17}$ cm^{-3}.

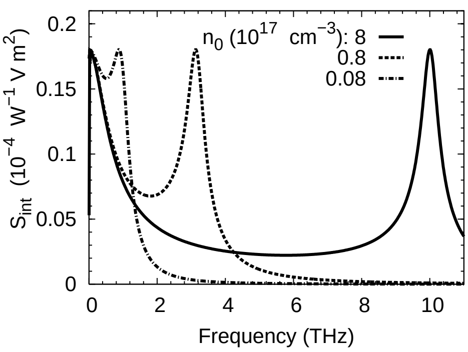

Figure 6: Intrinsic Responsivity S_{int} calculated for different electron concentration n_0 with $L = 400$ nm and $V_0 = 0.25$ Volt.

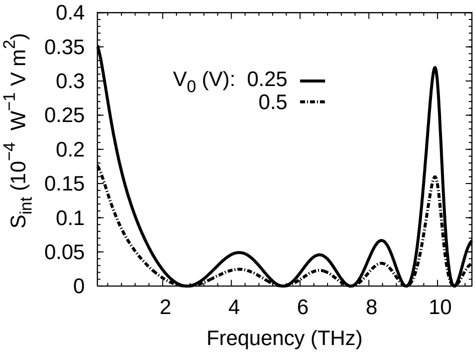

Figure 7: Intrinsic Responsivity S_{int} as functions of ac voltage component V_0. With $\omega_0 = 10$ GHz, $L = 400$ nm, $\nu = 3{\times}10^{12}$ s^{-1} and carrier concentration $n_0 = 8{\times}10^{17}$ cm^{-3}.

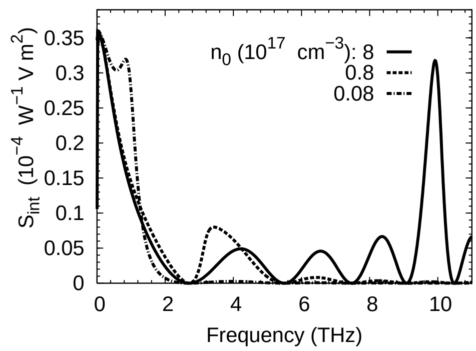

Figure 8: Intrinsic Responsivity S_{int} calculated for different electron concentration n_0 with applied voltage $V(t)$.

quency 10 THz corresponding to the presence of a resonance peak in real part of impedance (see figure 2). According to equation (4), the Responsivity behavior at low frequencies (Lorentzian form) and near 10 THz (resonance peak) depends to the two parts of ratio $\frac{V_0^2}{2Z(\omega)} = \frac{V_0^2}{2} Y(\omega)$ and $R(\omega) = Re[Z(\omega)]$, respectively. In addition, the decrease of the voltage to the value V_0 increases the amplitude of the Responsivity according to equation (4).

The effect of the electron concentration on the intrinsic Responsivity is reported in figure 6.

As discussed above (see figure 3), we remark the decreasing of the resonance peak to 1 THz corresponding to low electron concentration. This effect is related to the term ω_p.

Figure 7 reports the variation of the Responsivity $S_{int}(\omega)$ as a function of the ac voltage V_0 under a microwave voltage $V(t)$ applied between the diode terminals.

In the case presented in Fig. 7, a short series of peaks caused by the microwave excitation along to the diode is placed between the Lorentzian behavior and the resonance peak of 10 THz (see figure 3). Moreover, the small value of voltage V_0 leads to increase the amplitude of resonance peaks. As discussed above in Fig. 3, the most important resonance in the series of peaks (see figure 7) is at the frequency 10 THz where the impedance real part effect is dominant.

The Fig. 8 illustrates the carrier concentration effect on the intrinsic Responsivity for the microwave applied voltage $V(t)$.

In figure 8, the decreasing of carrier concentration of the diode leads to the disappearance of series peaks. This means that the low doped diode suppresses the frequency resonance and remains the Responsivity of diode to any harmonic signal neglected (see the concentration $8{\times}10^{15}$ cm^{-3} in figure 8).

4 Conclusion

An extension of analytical calculations based on the transistor model with the consideration distance channel-gate tends to infinity, is useful in this article to determine the impedance and the Responsivity of the nanochannel diodes. The calculation of the admittance elements leads to determine the complex impedance where thier real part presents the diode resistance. We have investigated the impedance as function of the diode parameters in the Terahertz range.

The impedance spectrum exhibits a peak near 10 THz corresponding to frequency plasma resonance. The appearance of the plasma resonance explains the behavior and the oscillation of electrons in the channel diode. The real part of impedance ($Re[Z(\omega)]$), on one hand, decreases when the length decrease, and on other hand, decreases by increasing the relaxation rate. We let not that has no effect of the diode geometry and of the relaxation rate on the resonance peak ω_p which depends only to the electron concentration. The discussion of the length and of the relaxation rate effects on the diode impedance leads to perform the diode geometry for a special frequency range detection or generation.

The intrinsic Responsivity S_{int} shows a significant dependence on the applied voltage according to their analytical expression. The Responsivity spectrum exhibits a Lorentzian form in low frequency and a resonance peak near 10 THz for a constant voltage applied between the diode terminals. A sinusoidal voltage applied to the diode introduces a supplementary resonances due to the harmonic contribution of the signal and leads to obtain a series of peaks in the intrinsic Responsivity spectrum. These peaks explain the frequencies detected or generated by the nanochannel diodes.

The carrier concentration can control the appearance of the frequency resonance and therefore the signal generated by the diode from an applied microwave voltage can be modified. As results, the low concentration near 10^{15} cm^{-3} suppresses the resonance peaks and down the intrinsic Responsivity of nanochannel diodes to applied signal.

Acknowledgements: The research was supported by the University of Montpellier, France in the case of the third author.

References:

[1] H. Marinchio, C. Palermo, L. Varani, P. Shiktorov, E. Starikov, and V. Gruzinskis, "Suppression of high-frequency electronic noise induced by 2d plasma waves in field-effect and high-electron-mobility transistors," *IEEE proceeding*, vol. DOI: 978-1-4577-0191-7/11, 2011.

[2] E. Starikov, P. Shiktorov, and V. Gružinskis, "Investigation of high-frequency small-signal characteristics of FETs/HEMTs," *Semicond. Sci. Technol.*, vol. 27, p. 045008, 2012.

[3] C. Balocco and al, "Room-temperature operation of a unipolar nanodiode at terahertz frequencies," *Journal of Applied Physics Letter*, vol. 98, p. 223501, 2011.

[4] I. Cortes-Mestizo, V. H. Mndez-Garca, J. Briones, M. P.-C. . R. Droopad, S. McMurtry, M. Hehn, F. Montaigne, and E. Briones, "Terahertz harvesting with shape-optimized inalas/ingaas self-switching nanodiodes," *AIP ADVANCES*, vol. 5, p. 117238, 2015.

[5] A. M. Song, M. Missous, A. R. Peaker, L. Samuelson, and W. Seifert, "Unidirectional electron flow in a nanometer-scale semiconductor channel: A self-switching device," *Applied Physics Letters*, vol. 83, p. 1881, September 2003.

[6] Y. Akbas, A. Stern, L. Q. Zhang, Y. Alimi, A. M. Song, I. de-la Torre, J. Mateos, T. Gonzlez, G. W. Wicks, and R. Sobolewski1, "Ultrahigh responsivity of optically active, semiconducting asymmetric nano-channel diodes," *IOP Publishing, Journal of Physics: Conference Series*, vol. 647, 2015.

[7] F. Z. Mahi, H. Marinchio, C. Palermo, and L. Varani, "Terahertz small-signal response of field-effect transistor channels," *IEEE Transactions On Terahertz Science And Technology*, vol. 5, pp. 584–589, JULY 2015.

[8] H. Marinchio, J.-F. Millithaler, C. Palermo, L. Varani, L. Reggiani, P. Shiktorov, E. Starikov, and V. Gružinskis, "Plasma resonances in a semiconductor slab of arbitrary thickness," *Appl. Phys. Lett.*, vol. 98, p. 203504, 2011.